JBUON 2021; 26(5): 1850-1861
ISSN: 1107-0625, online ISSN: 2241-6293 • www.jbuon.com
Email: editorial_office@jbuon.com

ORIGINAL ARTICLE

Circular RNA PRMT5 knockdown enhances cisplatin sensitivity and immune response in non-small cell lung cancer by regulating miR-138-5p/MYH9 axis

Yanping Xu*, Rongping Zhao*, Hua Wang, Jianwei Jiang, Zhenwei Wang, Jiayuan Wang, Wei Zhang, Min Li

Department of Laboratory Medicine, Renji Hospital, School of Medicine, Shanghai Jiao Tong University, Shanghai, China.

*Yanping Xu and Rongping Zhao contributed equally to this work and should be considered as co-first authors.

Summary

Purpose: *To explore the role and molecular mechanism of circRNA protein arginine methyltransferase-5 (circ-PRMT5) in regulating cisplatin (DDP) resistance and immune response of non-small cell lung cancer (NSCLC).*

Methods: *The expression of circ-PRMT5, miR-138-5p and myosin heavy chain 9 (MYH9) was determined by quantitative real-time polymerase chain reaction (qRT-PCR) and western blot analyses. Cell Counting Kit-8 (CCK-8) assay, flow cytometry, transwell assay, and western blot assay were utilized to evaluate DDP sensitivity. Interleukin 2 (IL-2), tumor necrosis factor alpha (TNF-a) and transforming growth factor β (TGF-β) production were measured by enzyme-linked immunosorbent assay (ELISA) to assess immune system's ability. A xenograft tumor model was established to explore the role of circ-PRMT5 in DDP resistance in vivo. The interaction between miR-138-5p and circ-PRMT5 or MYH9 was predicted by starBase and verified by dual-luciferase reporter assay.*

Results: *Circ-PRMT5 and MYH9 were upregulated and miR-138-5p was downregulated in DDP-resistant NSCLC tissues and cells. Circ-PRMT5 knockdown enhanced DDP sensitivity of NSCLC cells by inhibiting cell viability, migration and invasion and inducing apoptosis. Circ-PRMT5 knockdown also increased immune response by promoting the levels of IL-2 and TNF-a and decreasing the production of TGF-β. Moreover, circ-PRMT5 interference improved DDP sensitivity of NSCLC in vivo. MiR-138-5p was a direct target of circ-PRMT5 and its knockdown abated the effects of circ-PRMT5 downregulation on DDP resistance and immune response.*

Conclusion: *Circ-PRMT5 knockdown increased DDP sensitivity and immune response of NSCLC cells by regulating miR-138-5p/MYH9 axis, hinting potential value of circ-PRMT5 in the diagnosis and treatment for NSCLC.*

Key words: *non-small cell lung cancer, circ-PRMT5, miR-138-5p, MYH9, DDP resistance, immune response*

Introduction

Lung cancer is a frequent malignancy worldwide [1]. Non-small cell lung cancer (NSCLC) accounts for ~85% of lung cancer types, and 5-year survival rate for patients of all stages is only 15%[2].So far, many management strategies have been adopted in the treatment of NSCLC, such as surgery, chemotherapy, radiotherapy, immunotherapy, and some other targeted approaches [3]. Although cisplatin (DDP)-based chemotherapy is the most common strategy for treating NSCLC patients, the prognosis of NSCLC is poor because of drug resistance [4]. Immunotherapy represents a new approach for treating NSCLC and the goal of immunotherapy is to elevate the immune system's

Corresponding author: Min Li, Department of Laboratory Medicine, Renji Hospital, School of Medicine, Shanghai Jiao Tong University, 160 Pujian road, Shanghai200127, China.
Tel:+86-021-68383289; Email:limin1903@126.com
Received: 20/02/2021; Accepted: 02/04/2021

ability for detecting and eradicating tumor cells [5]. Combination of chemotherapy with immunotherapy is currently being studied in an attempt to further enhance the antineoplastic effect [6]. Hence, understanding the molecular mechanisms of DDP resistance and immune response in NSCLC is crucial to improve the outcome of NSCLC patients.

As a new kind of endogenous non-coding (nc) RNA, the functions of circular RNAs (circRNAs) have drawn widespread attention in the field of biology [7]. CircRNAs have covalently closed-loop structures without 5'-end cup and 3'-end ploy A tail, enabling them resistant to RNA exonuclease and more stable as well as difficult to degrade [8,9]. CircRNAs have been suggested to participate in the progression of cancers via modulation of cell proliferation, metastasis, and differentiation [10,11]. Moreover, it has been reported that circRNAs are involved in the chemoresistance of various cancers through promoting cell growth and decreasing apoptosis [12,13]. Besides, emerging evidence suggests that circRNAs may play pivotal roles in tumor immunity and immunotherapy [14]. A previous study indicated that circRNA protein arginine methyltransferase-5 (circ-PRMT5; hsa_circ_0031242, chr14:23389732-23392044) was derived from the PRMT5 gene and acted as an oncogene in NSCLC [15]. However, the functions of circ-PRMT5 in DDP resistance and immune response remain undetermined in NSCLC.

Up to now, the association between circRNAs and microRNAs (miRNAs) has drawn great attention. One popular hypothesis suggests that circRNAs can function as competing endogenous RNAs (ceRNAs; also known as miRNA sponges) to modulate the expression and activities of miRNAs, resulting in a change in the expression of miRNA target genes [16]. It had been proven that miR-138-5p was lowly expressed in DDP-resistant NSCLC tissue samples, and miR-138-5p participated in TRIM65-induced DDP resistance [17]. Hence, this research was designed to study whether the effects of circ-PRMT5 on DDP resistance and immune response were mediated by miR-138-5p in NSCLC. Besides, previous studies showed that myosin heavy chain 9 (MYH9) acted as a tumor promoter in several cancers, including NSCLC [18,19]. However, the functions of MYH9 on DDP resistance and immune response as well as the circ-PRMT5/miR-138-5p/MYH9 regulatory network in NSCLC have not been reported.

In this work, the abundance of circ-PRMT5, miR-138-5p and MYH9 in DDP-resistant NSCLC tissues and cells was detected. Furthermore, we explored the influence of circ-PRMT5, miR-138-5p and MYH9 on DDP resistance and immune response in NSCLC by gain- and loss-of-function experiments. Besides, we investigated whethercirc-PRMT5 could regulate MYH9 expression via sponging miR-138-5p. The aim of this research was to offer a promising therapeutic strategy for NSCLC patients with DDP resistance and enhance the immune system's ability.

Methods

Specimens collection

The clinical specimens including DDP-resistant and DDP-sensitive NSCLC tissues were acquired from patients who underwent surgery at Renji Hospital, School of Medicine, Shanghai Jiao Tong University. These tissues were divided into 2 groups: DDP-sensitive (n=30) group and DDP-resistant (n=30) group, according to the patient outcomes after DDP treatment. These tissues were harvested and timely frozen in liquid nitrogen, and then preserved at -80°C until use. These subjects provided informed consents before the study. This procedure was granted by the Ethics Committee of Renji Hospital, School of Medicine, Shanghai Jiao Tong University. Animal studies were performed in compliance with the ARRIVE guidelines and the Basel Declaration.

Cell culture and transfection

Human bronchial epithelial cell line (HBE1) and NSCLC cells (A549 and H1299) were obtained from BeNa Culture Collection (Beijing, China). To establish DDP-resistant NSCLC cell lines (A549/DDP and H1299/DDP), the parental cell lines (A549 and H1299) were initially exposed to 0.25 μM of DDP (Sigma, St. Louis, MO, USA) and then treated with a stepwise enhancing concentration of DDP until the final concentration of DDP was 2 μM. Moreover, 2 μM DDP was placed in culture medium ofDDP-resistant NSCLC cells to maintain the drug-resistant phenotype prior to further experiments. Cells were cultured in RPMI-1640 medium (Hyclone, Logan, UT, USA) containing 10% fetal bovine serum (FBS) (Invitrogen, Carlsbad, CA, USA) at 37°C in a moist incubator with 5% CO_2.

Small interfering RNA (siRNA) againstcirc-PRMT5 (si-circ-PRMT5) and siRNA negative control (si-NC), circ-PRMT5 or MYH9 overexpression plasmid (circ-PRMT5 or MYH9) and their negative control (pcDNA), mimic or inhibitor of miR-138-5p (miR-138-5p or anti-miR-138-5p) and matched negative controls (miR-NC or anti-miR-NC) were provided by Genechem (Shanghai, China). Lentivirus-mediated short hairpin RNA (shRNA) interference targeting circ-PRMT5 (sh-circ-PRMT5) and shRNA negative control (sh-NC) were provided by RiboBio (Guangzhou, China). Lipofectamine 3000 (Invitrogen) was utilized for cell transfection.

Quantitative real-time polymerase chain reaction (qRT-PCR)

TRIzol reagent (Invitrogen) was employed for isolating the total RNA from tissue samples or cell lines. The first strand of complementary DNA (cDNA) for circ-PRMT5, MYH9 and miR-138-5p wassynthesized with

the Prime Script RT reagent Kit (TaKaRa, Kusatsu, Japan) and TaqMan MicroRNA RT Kit (Thermo Fisher Scientific, Waltham, MA, USA). For detecting RNA levels, qRT-PCR reactions were performed on the 7500 real-time PCR systems (Thermo Fisher Scientific) using SYBR Green PCR Master Mix (Thermo Fisher Scientific). The change in gene expression was evaluated using the $2^{-\Delta\Delta Ct}$ method, followed by normalization to glyceraldehyde-3-phosphate dehydrogenase (GAPDH) or U6. Primers used for amplification were listed as follows: circ-PRMT5, 5'-TACCATTGGCCTCTAGCCCT-3' (F) and 5'-CAAGGGGAATCACAGCCCAT-3' (R); miR-138-5p, 5'-GCGAGCTGGTGTTGTGAATC-3' (F) and 5'- AGTGCAGGGTCCGAGGTATT-3' (R); MYH9, 5'-AGAGCTCACGTGCCTCAACG-3' (F) and 5'-TGACCACACAGAACAGGCCTG-3' (R); GAPDH, 5'-CGCTCTCTGCTCCTCCTGTTC-3' (F) and 5'-ATCCGTTGACTCCGACCTTCAC-3' (R); U6, 5'-CTCGCTTCGGCAGCACATATACT-3' (F) and 5'-ACGCTTCACGAATTTGCGTGTC-3' (R).

Cell counting kit-8 (CCK-8) assay

CCK-8 assay was used for measuring cell viability. Briefly, A549/DDP and H1299/DDP cells were placed in 96-well plates overnight. These cells were introduced with oligonucleotides and/or plasmids and then exposed to various concentrations of DDP for 48 h. Subsequently, CCK-8 solution (10 μL) (Boster, Wuhan, China) was added per well. Following incubation for 2 h, a microplate reader (Thermo Fisher Scientific) was employed to examine the absorbance per well at 450 nm.DDP concentration causing 50% inhibition of growth (IC_{50}) was measured according to the relative survival curve.

Apoptosis assay

Annexin V-fluorescein isothiocyanate (FITC)/propidium iodide (PI) apoptosis detection kit (Keygen, Nanjing, China) was applied for detecting cell apoptosis. In brief, cells were placed in six-well plates overnight. After that, these cells were introduced with oligonucleotides or/and plasmids for 48 h. Next, cells were harvested and washed, followed by staining with Annexin V-FITC and PIin the darkness for 20 min. Finally, the percentage of apoptotic cells in each sample was examined via a flow cytometer (Guava Technologies, Hayward, CA, USA).

Transwell assay

The 24-well transwell chambers (Corning Incorporation, Corning, NY, USA) were used for measuring cell migration and invasion. For cell migration, cells (5×10^4) resuspended in FBS-free medium (100 μL) were placed in top chambers. For cell invasion, cells resuspended in FBS-free medium (100 μL) were placed in top chambers pre-coated with Matrigel (BD Biosciences, San Jose, CA, USA). RPMI-1640 medium mixed with 10% FBS was placed into the bottom chamber. Non-migrated or non-invaded cells from top of the chamber were gently removed with cotton wool following incubation for 24 h. The migrated or invaded cells from lower of the chamber were fixed with paraformaldehyde (4%), followed by staining with crystal violet (0.1%). For quantification, a microscope (Olympus, Tokyo, Japan) was utilized to photograph and count the migrated and invaded cells.

Enzyme-linked immunosorbent assay (ELISA)

Pan T-Cell Isolation Kit II (Miltenyi BiotecInc., Auburn, CA) was employed to isolate human T-cells from healthy donor-derived peripheral blood mononuclear cells (PBMCs). T-cells were co-cultured with the A549/DDP and H1299/DDP cells at a 10:1 ratio. After transfection for 24 h, ELISA kits (Elabscience, Wuhan, China) were employed to assess the concentrations of IL-2, TNF-α and TGF-β in co-culture media. The data were presented in terms of pictogram (pg) per milliliter (mL).

Western blot assay

Total protein was extracted from tissue samples or cell lines by RIPA buffer (Solarbio, Beijing, China) mixed with 1 mM phenylmethylsulphonyi fluoride. Next, BCA protein assay kit (Tanon, Shanghai, China) was used for detection of protein concentration. Protein (about 40 μg) denatured at 98°C for 5 min was resolved bysodium dodecyl sulfate-polyacrylamide gel electrophoresis (SDS-PAGE), followed by transfer onto polyvinylidene fluoride (PVDF) membranes. After that, membranes would be blocked using5% skim milk (Yili, Beijing, China), and then probed with the primary antibody against P-glycoprotein (P-gp; 1:300; ab103477, Abcam, Cambridge, UK), multidrug resistance-associated protein 1 (MRP1; 1:500; ab32574, Abcam), MYH9 (1:500; ab241068, Abcam), or GAPDH (1:2000, ab37168, Abcam) overnight at 4°C . Afterward, HRP-linked goat anti-rabbit/mouse secondary antibodies (1:4000;ab205719/ab205718, Abcam) were utilized for further membrane incubation. The signal intensity was visualized with the enhanced chemiluminescence reagent (Tanon). Band density was analyzed with the ImageJ software, followed by normalizing to GAPDH expression.

Xenografted tumor model

BALB/c-nude mice (male, 4-5 weeks, 18-20 g, Huafukang Beijing, China) were randomly distributed into 2 groups (n=6/group), and subcutaneously injected with sh-circ-PRMT5- or sh-NC-transfected A549/DDP cells. After 7 days, nude mice were treated with DDP (5 mg/kg) or phosphate-buffered saline (PBS) every 4 days. The tumor sizes were determined by examining their length (L) and width (W) using a caliper every 4 days and tumor volume (V) was calculated with the following equation: $0.5\times L\times W^2$. These mice would be sacrificed following injection for 27 days, tumor samples were weighed and harvested for further analyses. The animal experiments obtained approval from the Animal Care and Use Committee of Renji Hospital, School of Medicine, Shanghai Jiao Tong University.

Dual-luciferase reporter assay

Interaction between miR-138-5p and circ-PRMT5 or MYH9 was predicted using the starBase. The fragments of circ-PRMT5 or MYH9 3'UTR that contained the predicted wild-type (WT) binding sites for miR-138-5p or mutant (MUT) miR-138-5p binding sites were synthesized and cloned into pmirGlO luciferase reporter vector (Promega, Madison, WI, USA), namely WT-circ-PRMT5, WT-MYH9 3'UTR, MUT-PRMT5, and MUT-MYH9 3'UTR.

We co-transfected one of reporter plasmids with miR-138-5p (or miR-NC) into A549-DDP and H1299-DDP cells for 48 h. Lastly, a dual-luciferase assay system (Promega) was applied for analyzing the luciferase activity.

Statistics

In this study, data were presented as mean± standard deviation (SD) from at least three independent experiments. Comparisons between groups were analyzed with Student's *t*-test (for 2 groups) or a one-way analysis of variance (ANOVA; for multiple groups). Correlation between miR-138-5p and circ-PRMT5 or MYH9was evaluated with Pearson correlation analysis. All statistical analyses were performed with the Graphpad Prism version 6.0 software. P<0.05 was considered to indicate statistical significance.

Results

Circ-PRMT5 was upregulated in DDP-resistant NSCLC tissues and cells

Firstly, the expression of circ-PRMT5 was detected in DDP-resistant NSCLC tissues and cells. Results of qRT-PCR indicated that the expression of circ-PRMT5 was higher in DDP-resistant NSCLC tissues than DDP-sensitive NSCLC tissues (Figure 1A). Similarly, the expression of circ-PRMT5 was enhanced in NSCLC cells (A549 and H1299) compared with HBE1 cells, and the level of circ-PRMT5 was significantly higher in DDP-resistant NSCLC cells (A549/DDP and H1299/DDP) than NSCLC cells (Figure 1B). These data suggested that the upregulation of circ-PRMT5 might be related to DDP resistance in NSCLC.

Knockdown of circ-PRMT5 enhanced DDP sensitivity and immune response in DDP-resistant NSCLC cells

To determine the biological functions of circ-PRMT5 in DDP-resistant NSCLC cells, we silenced circ-PRMT5 in A549/DDP and H1299/DDP cells by transfection with si-circ-PRMT5. To measure the transfection efficiency of si-circ-PRMT5, qRT-PCR was carried out. The results presented that transfection of si-circ-PRMT5 significantly reduced circ-PRMT5 expression in A549/DDP and H1299/DDP cells (Figure 2A). CCK-8 assay displayed that depletion of circ-PRMT5 decreased cell viability and IC_{50} value of DDP in A549/DDP and H1299/DDP cells (Figure 2B and 2C). Flow cytometry analysis showed that circ-PRMT5 deficiency promoted apoptosis of A549/DDP and H1299/DDP cells (Figure 2D). Transwell assay indicated that interference of circ-PRMT5 suppressed migration and invasion of A549/DDP and H1299/DDP cells (Figure 2E and 2F). T-cells are a major component of cellular immune response and are the essential cells required for anti-tumor immunity [20]. To determine the effect of circ-PRMT5 on immune response, ELISA analysis was performed in A549/DDP and H1299/DDP cells co-cultured with T-cells. IL-2 and TNF-a play critical roles in the activation of immune system that could be a useful way to eradicate cancer, while TGF-β can act as an immunosuppressive cytokine and increasing expression of TGF-β allows immunogenic cell lines to escape immunosurveillance and form tumors [21,22]. The results showed that silence of circ-PRMT5 increased the levels of IL-2 and TNF-a while decreased the production of TGF-β (Figure 2G), implying that circ-PRMT5 knockdown might activate the T-cell immune response during chemotherapy of DDP. To identify drug resistance associated-proteins, the expression levels of P-gp and MRP1 were analyzed by western blot assay in A549/DDP and H1299/DDP cells. As illustrated in Figure 2H and 2I, circ-PRMT5 downregulation reduced the protein levels of P-gp and MRP1. Taken together, these data suggested that circ-PRMT5 knockdown improved the sensitivity of DDP and activated T-cell immune response.

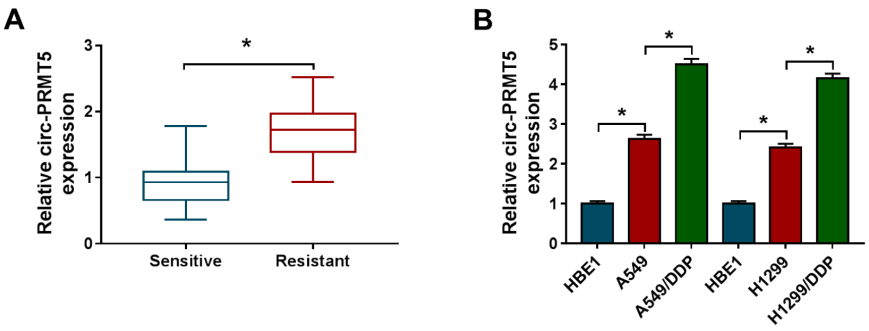

Figure 1. Circ-PRMT5 was highly expressed in DDP-resistant NSCLC tissues and cells. **A:** The expression of circ-PRMT5 was detected by qRT-PCR in DDP-resistant and DDP-sensitive NSCLC tissues. **B:** The level of circ-PRMT5 was measured by qRT-PCR in HBE1 cells, NSCLC cells (A549 and H1299) and DDP-resistant NSCLC cells (A549/DDP and H1299/DDP) (*p<0.05).

Downregulation of circ-PRMT5 inhibited tumor growth and increased DDP sensitivity in vivo

To explore whether knockdown of circ-PRMT5 affected DDP resistance *in vivo*, sh-NC- or sh-circ-PRMT5-transfected A549/DDP cells were subcutaneously injected into BALB/c nude mice and then treated with DDP. The images of tumor tissues are presented in Figure 3A. As shown in Figure 3B and 3C, the tumor volume and tumor weight were inhibited in the sh-circ-PRMT5 + DDP group compared with sh-NC + DDP group. The results of qRT-PCR displayed that the expression of circ-PRMT5 was lower in sh-circ-PRMT5 + DDP group than sh-NC + DDP group (Figure 3D). These findings indicated that circ-PRMT5 knockdown might enhance the sensitivity of DDP to inhibit tumor growth *in vivo*.

Circ-PRMT5 directly targeted miR-138-5p and negatively regulated the expression of miR-138-5p

CircRNAs were found to act as molecular sponges of miRNAs to regulate miRNA targets [23]. Therefore, the potential interactions between miRNAs and circ-PRMT5 were investigated in this research. Through starBase prediction, miR-138-5p was predicted as a potential target of circ-PRMT5 (Figure 4A). To confirm the association between miR-138-5p and circ-PRMT5, we performed dual-luciferase reporter assay. The results showed that miR-138-5p overexpression suppressed the luciferase activity of WT-circ-PRMT5, but did not change the luciferase activity of MUT-circ-PRMT5 in A549/DDP and H1299/DDP cells (Figure 4B and 4C). Next, the expression of miR-138-5p was examined in DDP-resistant and DDP-sensitive NSCLC tissues.

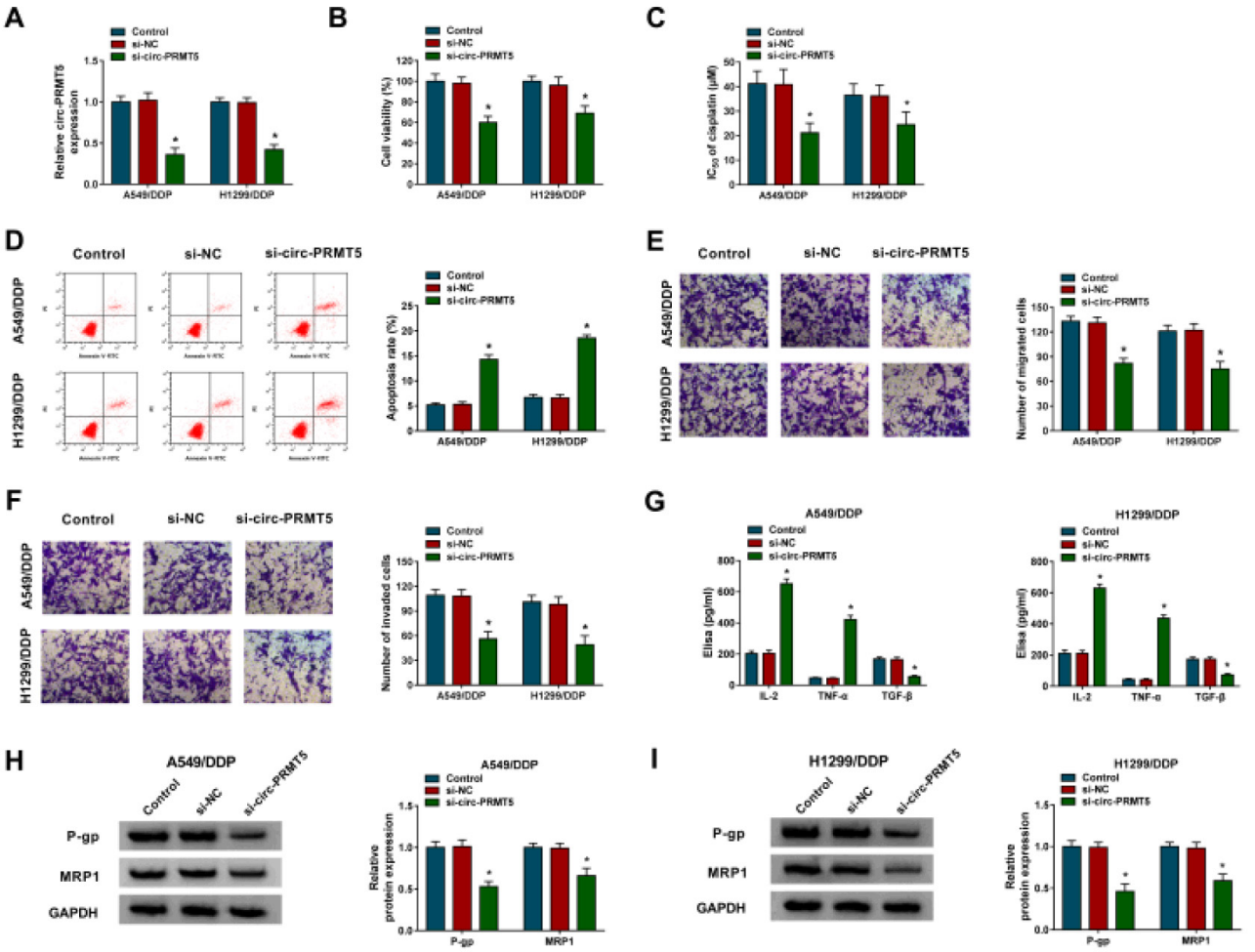

Figure 2. Knockdown of circ-PRMT5 sensitized DDP-resistant NSCLC cells to DDP and enhanced immune response. A549/DDP and H1299/DDP cells were transfected with si-NC or si-circ-PRMT5, and un-transfected cells were regarded as the control group. **A:** Knockdown efficiency of circ-PRMT5 was determined by qRT-PCR. **B and C:** The cell viability and IC_{50} value of DDP were measured using CCK-8 assay. **D:** Flow cytometry analysis was applied to detect cell apoptosis. **E and F:** Transwell assay was used to measure the migration and invasion abilities (100×). **G:** The concentrations of IL-2, TNF-α and TGF-β were determined by ELISA in the co-culture supernatants of DDP-resistant NSCLC cells and T-cells. **H and I:** Western blot assay was conducted to examine the protein levels of P-gp and MRP1(*p<0.05).

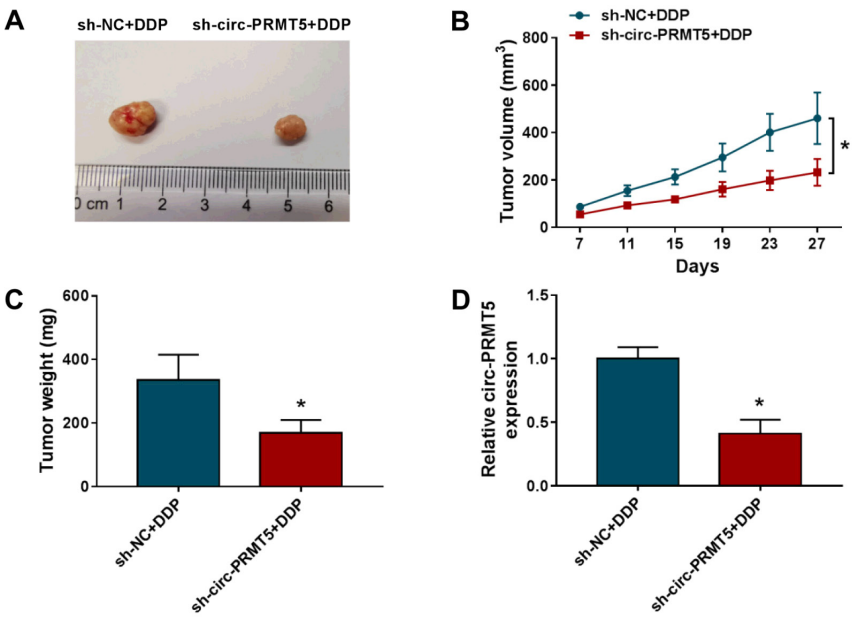

Figure 3. Downregulation of circ-PRMT5 enhanced the sensitivity of DDP by inhibiting tumor growth *in vivo*. Sh-NC- or sh-circ-PRMT5-transfected A549/DDP cells were subcutaneously injected into BALB/c nude mice and then exposed to DDP (5 mg/kg). **A:** Representative images of xenograft tumors were presented. **B and C:** The growth curves and weight of xenograft tumors were shown. **D:** Circ-PRMT5 expression was measured by qRT-PCR in dissected tumor tissues (*p<0.05).

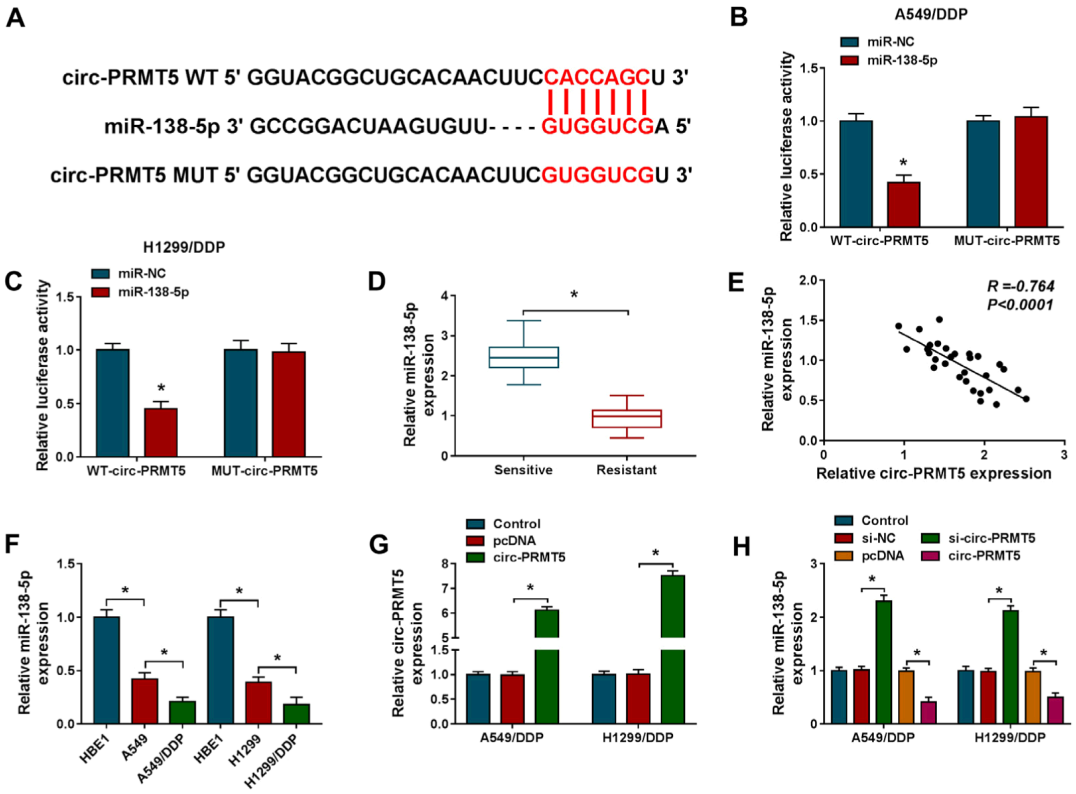

Figure 4. MiR-138-5p was a direct target of circ-PRMT5. **A:** Binding region between circ-PRMT5 and miR-138-5p, and matched mutant sites were displayed. **B and C:** The luciferase activity was detected by dual-luciferase reporter assay in A549/DDP and H1299/DDP cells co-transfected with luciferase reporter plasmids (WT-circ-PRMT5 or MUT-circ-PRMT5) and miR-NC ormiR-138-5p. **D:** The expression of miR-138-5p was analyzed using qRT-PCR in DDP-sensitive andDDP-resistant NSCLC tissues. **E:** Correlation between miR-138-5p and circ-PRMT5 was analyzed in DDP-resistant NSCLC tissues. **F:** The expression of miR-138-5p was determined by qRT-PCR in HBE1 cells, NSCLC cells (A549 and H1299) and DDP-resistant NSCLC cells (A549/DDP and H1299/DDP). **G:** Overexpression efficiency of circ-PRMT5 was examined by qRT-PCR in A549/DDP and H1299/DDP cells. **H:** The expression of miR-138-5p was measured by qRT-PCR in control cells (A549/DDP and H1299/DDP) or those cells transfected with si-NC, si-circ-PRMT5, pcDNA, or circPRMT5 (*p<0.05).

The results indicated that miR-138-5p level was remarkably decreased in DDP-resistant NSCLC tissues relative to DDP-sensitive NSCLC tissues (Figure 4D).Pearson correlation analysis showed that miR-138-5p expression was negatively correlated with circ-PRMT5 level in DDP-resistant NSCLC tissues (Figure 4E). Likewise, the expression of miR-138-5p was decreased in NSCLC cells (A549 and H1299) compared to that in HBE1 cells, and the level of miR-138-5p was significantly reduced in DDP-resistant NSCLC cells (A549/DDP and H1299/DDP) in contrast to NSCLC cells (A549 and H1299) (Figure 4F). The transfection efficiency of circ-PRMT5 was analyzed by the qRT-PCR assay. The results showed that circ-PRMT5 expression was obviously increased in A549/DDP and H1299/DDP cells transfected with circ-PRMT5 compared with those cells transfected with pcDNA or control group (Figure 4G). Subsequently, we explored the effect of circ-PRMT5 on the expression of miR-138-5p. As depicted in Figure 4H, knockdown of circ-PRMT5 promoted the expression of miR-138-5p, while overexpression of circ-PRMT5 inhibited the expression of miR-138-5p. Overall, these data revealed that miR-138-5p was a direct target of circ-PRMT5.

Circ-PRMT5 interference promoted DDP sensitivity and immune response by upregulating miR-138-5p in DDP-resistant NSCLC cells

To explore whether circ-PRMT5 exerted its biological functions by sponging miR-138-5p, rescue experiments were performed in which DDP-resistant NSCLC cells were transfected with si-NC, si-circ-PRMT5, si-circ-PRMT5 + anti-miR-NC, or si-circ-PRMT5 + anti-miR-138-5p. We found that the expression of miR-138-5p was increased after knockdown of circ-PRMT5 in A549/DDP and H1299/DDP cells, which was abated by downregulating miR-138-5p (Figure 5A). Moreover, the inhibitory effects of circ-PRMT5 downregulation on cell viability and IC_{50} value of DDP were abolished by knockdown of miR-138-5p (Figure 5B and 5C). Fur-

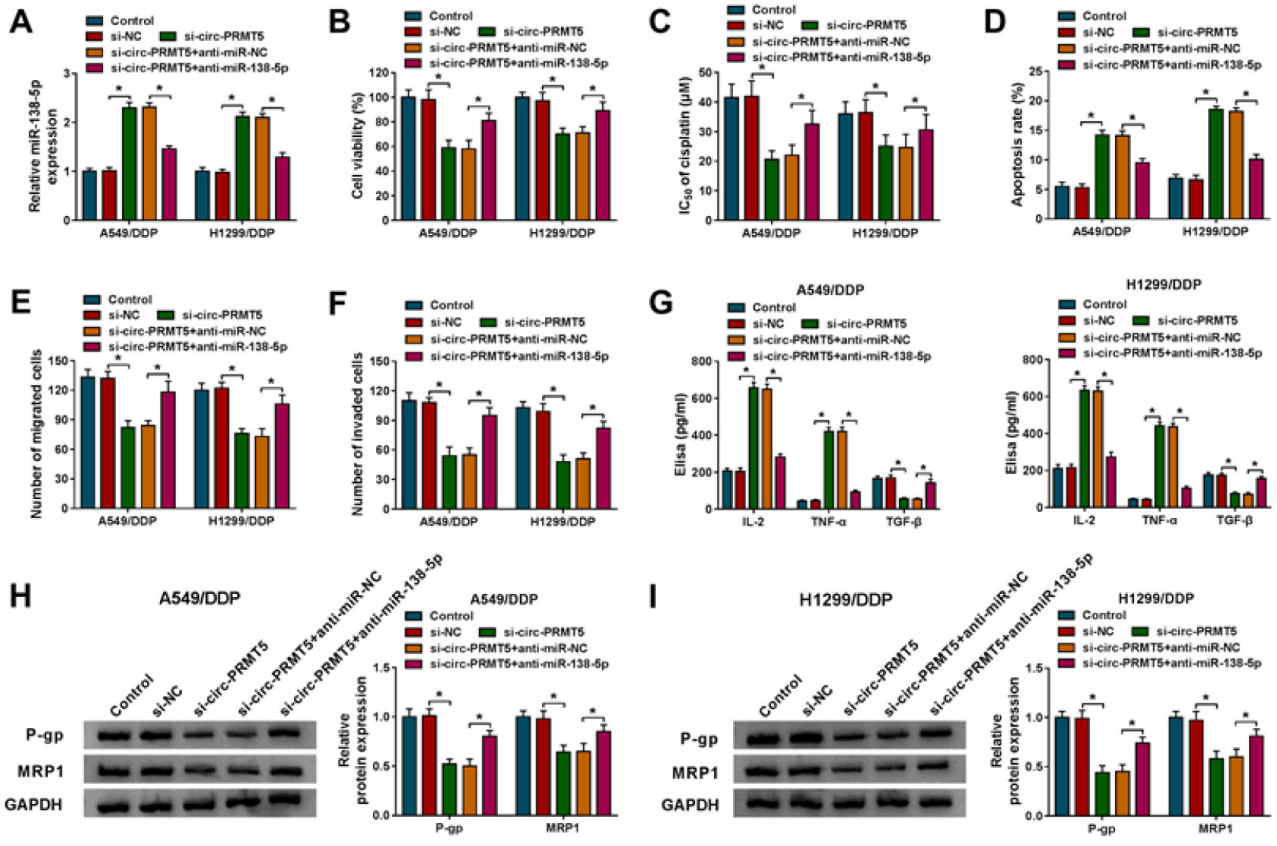

Figure 5. Circ-PRMT5 knockdown enhanced DDP sensitivity of NSCLC cells and immune response by upregulating miR-138-5p. A549/DDP and H1299/DDP cells were transfected with si-NC, si-circ-PRMT5, si-circ-PRMT5 + anti-miR-NC, si-circ-PRMT5 + anti-miR-138-5p, and un-transfected cells were regarded as the control group. **A:** MiR-138-5p expression was measured using the qRT-PCR analysis. **B and C:** The cell viability and IC_{50} value of DDP were determined by CCK-8 assay. **D:** Cell apoptosis was examined using flow cytometry analysis. **E and F:** Transwell assay was utilized to assess cell migration and invasion abilities (100×). **G:** IL-2, TNF-α and TGF-β secretion in co-culture supernatants of DDP-resistant NSCLC cells and T-cells were determined by ELISA. **H and I:** The protein levels of P-gp and MRP1 were detected by western blot assay (*p<0.05).

thermore, downregulation of miR-138-5p mitigated si-circ-PRMT5-induced apoptosis in A549/DDP and H1299/DDP cells (Figure 5D). In addition, miR-138-5p interference could reverse the anti-migration and anti-invasion effects caused by knockdown of circ-PRMT5 (Figure 5E and 5F). Meanwhile, the effects of si-circ-PRMT5 on promotion of IL-2 and TNF-a levels and suppression of TGF-β secretion were abrogated by downregulatingmiR-138-5p (Figure 5G). Besides, the suppressive impact of circ-PRMT5 deficiency on the protein expression of P-gp and MRP1 was abated by interference of miR-138-5p (Figure 5H and 5I). Collectively, our results indicated that circ-PRMT5 exerted its biological functions through sponging miR-138-5p.

MYH9 was a downstream target of miR-138-5p

To further elucidate the mechanism of miR-138-5p, target prediction was performed by starBase. According to the starBase prediction, we found putative binding sites between MYH9 and miR-138-5p (Figure 6A), implying that miR-138-5p might direct target MYH9. We performed dual-luciferase reporter assay to validate this prediction. The results revealed that miR-138-5p overexpression could reduce the luciferase activity of WT-MYH9 3'UTR, which could not be observed in the MUT-MYH9 3'UTR group (Figure 6B). Subsequently, we examined the mRNA and protein levels of MYH9 in DDP-resistant and DDP-sensitive NSCLC tissues. As presented in Figures 6C and 6D, the

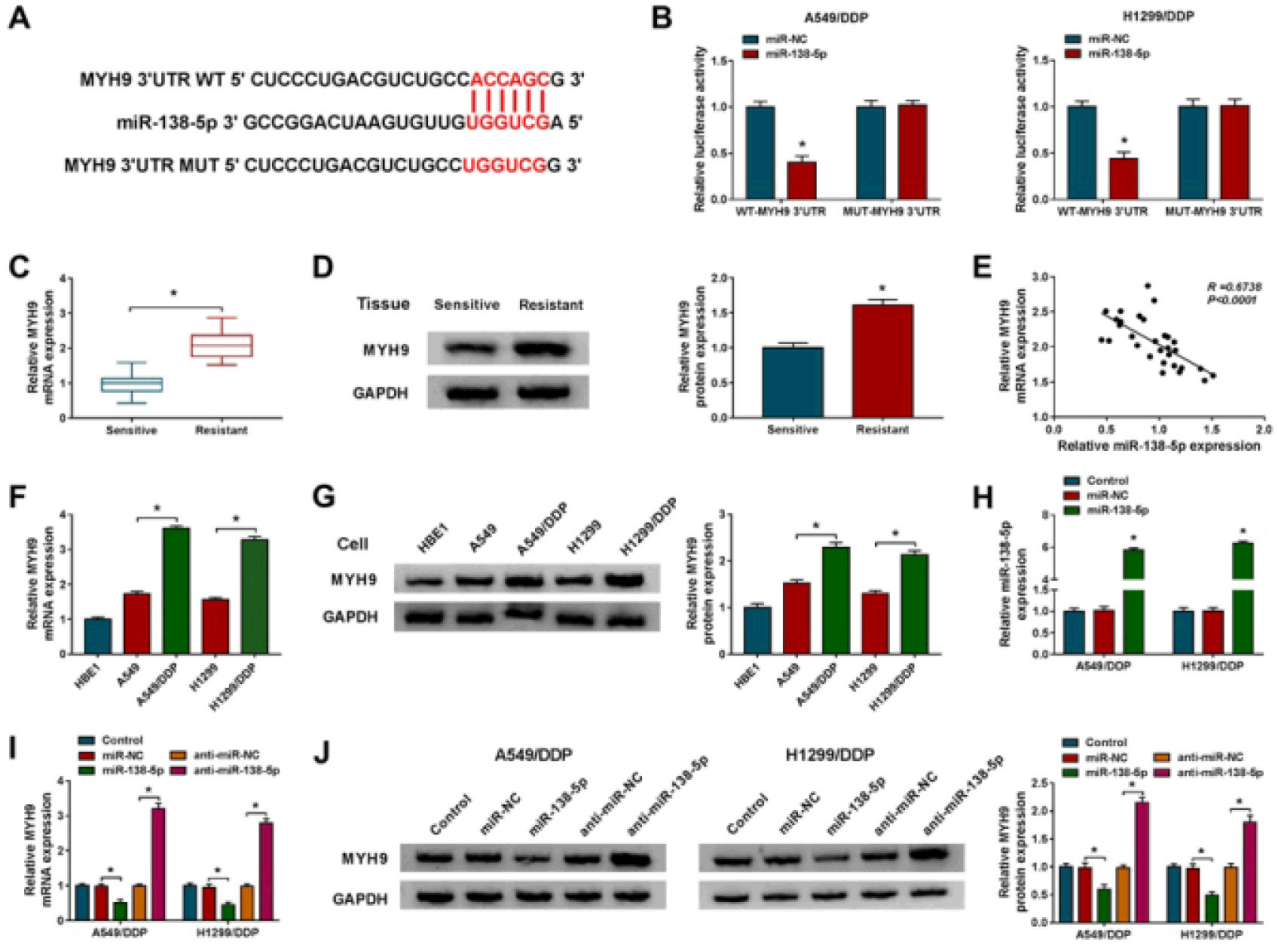

Figure 6. MYH9 was a direct target of miR-138-5p. **A:** The complementary sequences between MYH9 and miR-138-5p, as well as mutated nucleotides of MYH9 3'UTR were shown. **B:** Relative luciferase activity was determined in A549/DDP and H1299/DDP cells co-transfected withWT-MYH9 3'UTR or MUT-MYH9 3'UTR and miR-138-5p or miR-NC. **C and D:** The mRNA and protein expression of MYH9 were measured by qRT-PCR and western blot analyses, respectively, in DDP-sensitive andDDP-resistant NSCLC tissues. **E:** Correlation between MYH9 and circ-PRMT5 was analyzed in DDP-resistant NSCLC tissues. **F and G:** The qRT-PCR and western blot analyses were conducted to assess the mRNA and protein expression of MYH9 in HBE1 cells, NSCLC cells (A549 and H1299) and DDP-resistant NSCLC cells (A549/DDP and H1299/DDP). **H:** The qRT-PCR was applied to determine the overexpression efficiency of miR-138-5p in A549/DDP and H1299/DDP cells. **I and J:** The mRNA and protein expression of MYH9 were measured by qRT-PCR and western blot analyses, respectively, in control cells (A549/DDP and H1299/DDP) or those cells transfected with miR-NC, miR-138-5p, anti-miR-NC, or anti-miR-138-5p (*p<0.05).

mRNA expression and protein expression of MYH9 were both enhanced in DDP-resistant NSCLC tissues compared to DDP-sensitive NSCLC tissues. Moreover, the mRNA expression of MYH9 was inversely associated with the expression of miR-138-5p (Figure 6E). Similarly, the mRNA level and protein level of MYH9 were higher in DDP-resistant NSCLC cells than NSCLC cells (Figures 6F and 6G). The results of qRT-PCR indicated that miR-138-5p was successfully overexpressed in A549/DDP and H1299/DDP cells transfected with miR-138-5p (Figure 6H). Next, the effect of miR-138-5p on the expression of MYH9 was explored. The qRT-PCR and western blot analyses demonstrated that overexpression of miR-138-5p inhibited the mRNA expression and protein expression of MYH9, while knockdown of miR-138-5p presented an opposite effect (Figures 6I and 6J). Above all, these data proved that miR-138-5p could bind to MYH9.

Overexpression of miR-138-5p increased DDP sensitivity and immune response by downregulating MYH9 in DDP-resistant NSCLC cells

Transfection efficiency of MYH9 was determined by qRT-PCR and western blot analyses. As shown in Figures 7A and 7B, transfection of MYH9 markedly increased the mRNA level and protein level of MYH9, suggesting that MYH9 was successfully transfected into A549/DDP and H1299/DDP cells. To investigate whether MYH9 was involved

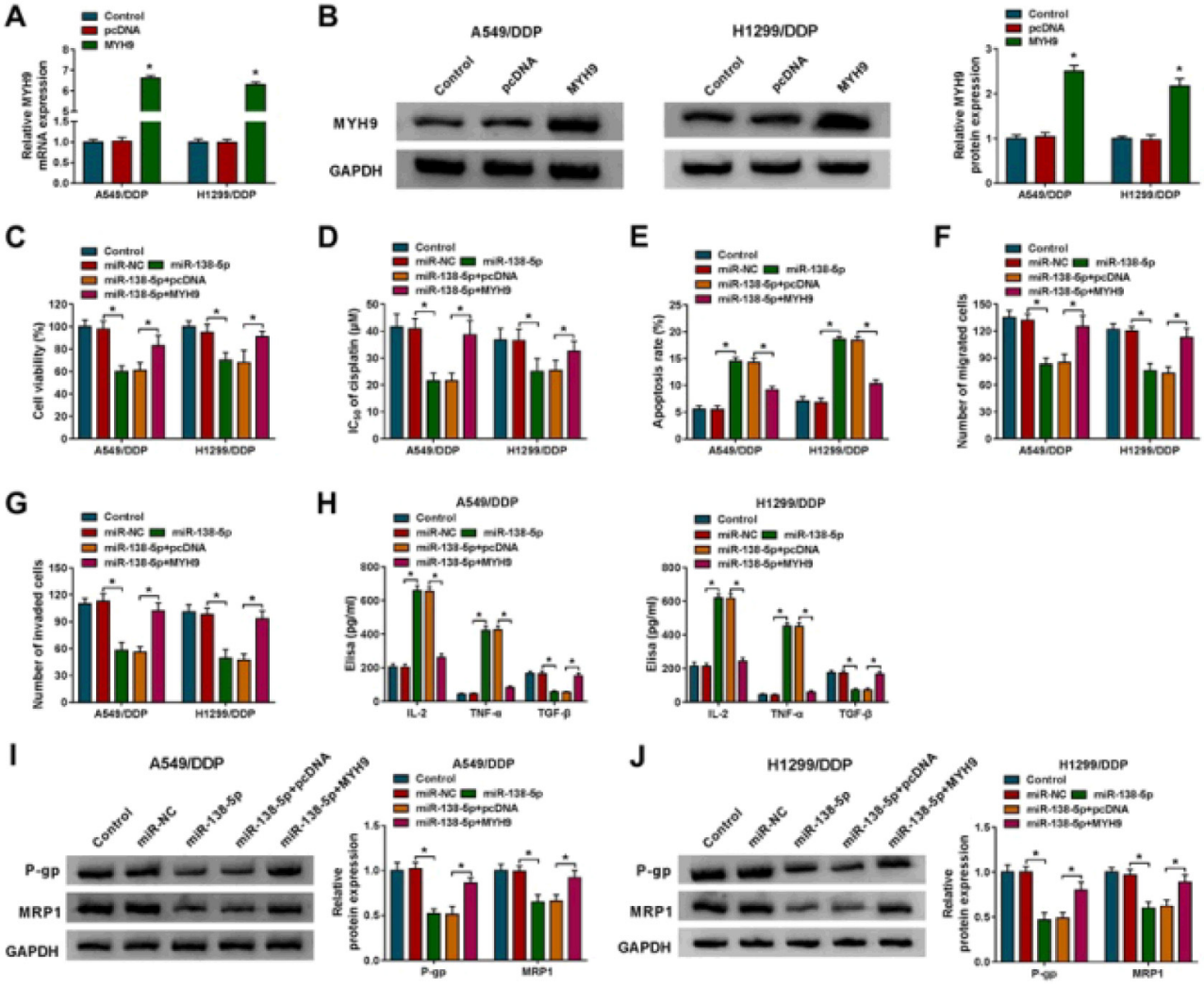

Figure 7. Upregulation of miR-138-5p enhanced immune response and DDP sensitivity of DDP-resistant NSCLC cells through inhibiting MYH9 expression. **A and B:** Transfection efficiency of MYH9 was determined by qRT-PCR and western blot analyses in A549/DDP and H1299/DDP cells. (C-J) A549/DDP and H1299/DDP cells were transfected with miR-NC, miR-138-5p, miR-138-5p + pcDNA, miR-138-5p + MYH9, and un-transfected cells were regarded as the control group. **C and D:** CCK-8 assay was performed for examining the cell viability and IC_{50} value of DDP. **E:** Cell apoptosis was determined using flow cytometry analysis. **F and G:** Transwell assay was employed to count the number of migrated or invaded cells (100×). **H:** IL-2, TNF-α and TGF-β production in co-culture supernatants of DDP-resistant NSCLC cells and T-cells were measured by ELISA. **I and J:** Western blot assay was used to measure the protein levels of P-gp and MRP1 (*p<0.05).

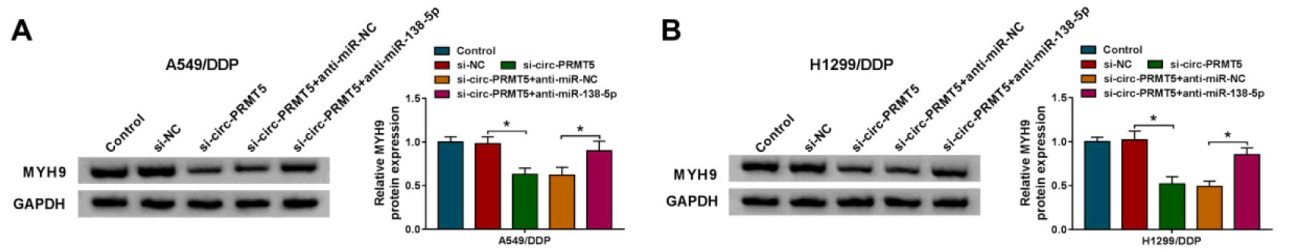

Figure 8. Circ-PRMT5 positively regulated MYH9 expression by sponging miR-138-5p. **A and B:** Western blot assay was carried out for detecting the protein expression of MYH9 in A549/DDP and H1299/DDP cells transfected with si-NC, si-circ-PRMT5, si-circ-PRMT5 + anti-miR-NC, or si-circ-PRMT5 + anti-miR-138-5p (*p<0.05).

in miR-138-5p-mediated functions, A549/DDP and H1299/DDP cells were transfected with miR-NC, miR-138-5p, miR-138-5p + pcDNA, miR-138-5p + MYH9. Overexpression of miR-138-5p inhibited cell viability and IC_{50} value of DDP, and accelerated cell apoptosis in A549/DDP and H1299/DDP cells, which these effects were abated by upregulation of MYH9 (Figures 7C-7E). Moreover, restoration of miR-138-5p resulted in inhibition of cell migration and invasion, while upregulation of MYH9 promoted migration and invasion of A549/DDP and H1299/DDP cells (Figures 7F and 7G). Additionally, overexpression of miR-138-5p increased IL-2 and TNF-a secretion and decreased TGF-β secretion, which was abolished by addition of MYH9 (Figure 7H). Furthermore, the protein levels of P-gp and MRP1 were reduced in A549/DDP and H1299/DDP cells transfected with miR-138-5p, while this effect was reversed by co-transfection of MYH9 (Figures 7I and 7J). Therefore, we concluded that miR-138-5p exerted its biological functions by targeting MYH9.

Circ-PRMT5 regulated MYH9 by acting as a molecular sponge of miR-138-5p

To validate whether circ-PRMT5 served as a molecular sponge of miR-138-5p to regulate the expression of MYH9, A549/DDP and H1299/DDP cells were transfected with si-NC, si-circ-PRMT5, si-circ-PRMT5 + anti-miR-NC, or si-circ-PRMT5 + anti-miR-138-5p. Western blot assay suggested that the protein expression of MYH9 was reduced in the si-circ-PRMT5 group compared to that in the si-NC group or control group and was then restored by the anti-miR-138-5p in A549/DDP and H1299/DDP cells (Figures 8A and 8B). These results suggested that silence of circ-PRMT5 inhibited MYH9 expression through regulating miR-138-5p.

Discussion

Although DDP is a commonly used chemotherapy drug against NSCLC, the development of chemoresistance has become a major obstacle to the successful treatment of NSCLC patients [24]. Increasing evidence has shown that dysregulation of circRNAs participates in chemoresistance of tumors and offers novel insights into the biology of cancer progression [25]. The immune system affects the development of cancers by acting as an extrinsic tumor suppressor, which can destroy developing tumors or restrain tumor expansion [26]. However, development of resistance of tumor cells can induce multiple changes in their immunobiological properties, which may enable tumor cells to escape immune surveillance and promote cancer progression [27,28]. In this research, we aimed to probe the function and underlying mechanism of circ-PRMT5 in DDP resistance and immune response.

Previous studies indicate that circRNAs are extensively expressed in eukaryotic cells and play pivotal roles in modulating multiple biological and pathological processes as well as the development of drug resistance [29]. Circ-PRMT5 has been revealed to be overexpressed and play an oncogenic role in certain human tumors, including bladder cancer, hepatocellular carcinoma and gastric cancer [30-32]. More importantly, a previous report showed that high abundance of circ-PRMT5 was observed in NSCLC tissues and cells, and its downregulation repressed NSCLC cell growth [15]. Nevertheless, the biological functions of circ-PRMT5 in chemoresistance and immune response have not been clarified. Here, we proved that circ-PRMT5 abundance was enhanced in DDP-resistant NSCLC tissues and cells, and its downregulation enhanced the sensitivity of DDP through inhibiting proliferation, migration, invasion, the expression of P-gp and MRP1, as well as promoting apoptosis in DDP-resistant NSCLC cells *in vitro*. Consistently, knockdown of circ-PRMT5 also increased the sensitivity of DDP by suppression of tumor growth *in vivo*. Additionally, we demonstrated that interference of circ-PRMT5 could elevate immune system's ability by promoting the levels of IL-2 and TNF-a as well as inhibiting the production of TGF-β. These

results revealed that circ-PRMT5 downregulation sensitized DDP-resistant NSCLC cells to DDP and increased immune system's ability, and increasing the immune response might help improve DDP sensitivity.

It has been proposed that circRNAs may exert their biological functions through acting as miRNA sponges [33]. To explore whether circ-PRMT5 acted as a miRNA sponge, bioinformatics analysis was performed. MiR-138-5p was predicted as a target of circ-PRMT5, which was validated through dual-luciferase reporter assay. MiR-138-5p has been suggested to serve as an anti-oncogene in many malignancies, including NSCLC [34,35]. Recent studies reported that miR-138-5p could regulate drug resistance in NSCLC [36,37]. Besides, miR-138-5p was demonstrated to be downregulated in DDP-resistant NSCLC tissues, and its interference could abate the functions of TRIM65 downregulation on autophagy and DDP-induced apoptosis [17]. In line with previous studies, we uncovered that miR-138-5p level was remarkably reduced in DDP-resistant NSCLC tissue samples and cell lines, and a negative correlation between miR-138-5p and circ-PRMT5 was observed. Besides, miR-138-5p interference could abolish the effects of circ-PRMT5 depletion on promotion of immune response and DDP sensitivity. These data indicated that circ-PRMT5 exerted its biological roles in DDP-resistant NSCLC cells through regulating miR-138-5p.

MiRNAs are known to participate in many physiological and pathological procedures through modulating the expression of target mRNAs [38-40]. Next, the candidate target genes of miR-138-5p were searched by starBase. Subsequently, the results proved that MYH9 was a downstream target of miR-138-5p. MYH9 has been suggested as a critical player in the progression of diverse tumors, including gastric cancer, hepatocellular carcinoma and ovarian cancer [41-43]. Also, some studies pointed out that MYH9 expression was an indicator of poor survival for NSCLC patients, and MYH9 knockdown inhibited NSCLC cell migration and invasion [19, 44]. Here, we observed that MYH9 level was elevated in DDP-resistant NSCLC tissues and cells, and negatively associated with miR-138-5p abundance in DDP-resistant NSCLC tissues. Moreover, MYH9 upregulation abolished the promotive impact of miR-138-5p restoration on DDP sensitivity and immune response. Furthermore, circ-PRMT5 could serve as a ceRNA of miR-138-5p to modulate MYH9 level. Collectively, these results implied that circ-PRMT5 regulated DDP resistance and immune response by modulating miR-138-5p/MYH9 axis.

In summary, our study demonstrated that circ-PRMT5 knockdown increased DDP sensitivity and immune response in DDP-resistant NSCLC cells via modulating miR-138-5p/MYH9 axis. Thus, our research contributes to better understanding of the molecular mechanism of chemoresistance and immune response in NSCLC, which might provide a promising circRNA-targeted therapy for NSCLC.

Conflict of interests

The authors declare no conflict of interests.

References

1. Torre LA, Bray F, Siegel RL, Ferlay J, Lortet-Tieulent J, Jemal A. Global cancer statistics, 2012. CA Cancer J Clin 2015;65:87-108.
2. Siegel R, Naishadham D, Jemal A. Cancer statistics, 2012. CA Cancer J Clin 2019;69:7-34.
3. Hirsch FR, Suda K, Wiens J, Bunn PA Jr. New and emerging targeted treatments in advanced non-small-cell lung cancer. Lancet 2016;388:1012-24.
4. Chang A. Chemotherapy, chemoresistance and the changing treatment landscape for NSCLC. Lung Cancer 2011;71:3-10.
5. Hall RD, Gray JE, Chiappori A A. Beyond the standard of care: a review of novel immunotherapy trials for the treatment of lung cancer. Cancer Control 2013;20:22-31.
6. Dasanu CA, Sethi N, Ahmed N. Immune alterations and emerging immunotherapeutic approaches in lung cancer. Expert Opin Biol Ther 2012;12:923-37.
7. Li X, Yang L, Chen LL. The biogenesis, functions, and challenges of circular RNAs. Molecular Cell 2018;71:428-42.
8. Memczak S, Jens M, Elefsinioti A et al. Circular RNAs are a large class of animal RNAs with regulatory potency. Nature 2013;495:333-8.
9. Chen LL, Yang L. Regulation of circRNA biogenesis. RNA Biol 2015;12:381-8.
10. Qin M, Liu G, Huo X, et al. Hsa_circ_0001649: a circular RNA and potential novel biomarker for hepatocellular carcinoma. Cancer Biomark 2016;16:161-9.
11. Meng S, Zhou H, Feng Z et al. CircRNA: functions and properties of a novel potential biomarker for cancer. Mol Cancer 2017;16:94.
12. Wang Y, Zhang L, Zheng X et al. Long non-coding RNA LINC00161 sensitises osteosarcoma cells to cisplatin-induced apoptosis by regulating the miR-645-IFIT2 axis. Cancer Lett 2016;382:137-46.

13. Yu W, Peng W, Sha H et al. Hsa_circ_0003998 promotes chemoresistance via modulation of miR-326 in lung adenocarcinoma cells. Oncol Res 2019;27:623-8.
14. Xu Z, Li P, Fan L, Wu M. The potential role of circRNA in tumor immunity regulation and immunotherapy. Front Immunol 2018;9:9.
15. Wang Y, Li Y, He H, Wang F. Circular RNA circ-PRMT5 facilitates non-small cell lung cancer proliferation through upregulating EZH2 via sponging miR-377/382/498. Gene 2019;720:144099.
16. Hansen TB, Jensen TI, Clausen BH et al. Natural RNA circles function as efficient microRNA sponges. Nature 2013 495:384-8.
17. Pan X, Chen Y, Shen Y, Tantai J. Knockdown of TRIM65 inhibits autophagy and cisplatin resistance in A549/DDP cells by regulating miR-138-5p/ATG7. Cell Death Dis 2019;10:429.
18. Wang B, Qi X, Liu J et al. MYH9 promotes growth and metastasis via activation of MAPK/AKT signaling in colorectal cancer. J Cancer 2019;10:874-84.
19. Lin HC, Zhang FL, Geng Q et al. Quantitative proteomic analysis identifies CPNE3 as a novel metastasis-promoting gene in NSCLC. J Proteome Res 2013;12:3423-33.
20. Ostrand-Rosenberg S. CD4+ T lymphocytes: a critical component of antitumor immunity. Cancer Invest 2005;23:413-9.
21. Jiang T, Zhou C, Ren S. Role of IL-2 in cancer immunotherapy. Oncoimmunology 2016;5:e1163462.
22. Elliott RL, Blobe GC. Role of transforming growth factor Beta in human cancer. Hum Vaccin Immunother 2017;13:1741-50.
23. Kulcheski FR, Christoff AP, Margis R. Circular RNAs are miRNA sponges and can be used as a new class of biomarker. J Biotechnol 2016;238:42-51.
24. Cao L, Chen J, Ou B et al. GAS5 knockdown reduces the chemo-sensitivity of non-small cell lung cancer (NSCLC) cell to cisplatin (DDP) through regulating miR-21/PTEN axis. Biomed Pharmacother 2017;93:570-9.
25. Xue M, Li G, Fang X et al. hsa_circ_0081143 promotes cisplatin resistance in gastric cancer by targeting miR-646/CDK6 pathway. Cancer Cell Int 2019;19:25.
26. Gubin M M, Zhang X, Schuster H et al. Checkpoint blockade cancer immunotherapy targets tumour-specific mutant antigens. Nature 2014;515:577-81.
27. Chacon JA, Schutsky K, Powell DJ. The impact of chemotherapy, radiation and epigenetic modifiers in cancer cell expression of immune inhibitory and stimulatory molecules and anti-tumor efficacy. Vaccines (Basel) 2016;4:43.
28. Wicki A, Mandalà M, Massi D et al. Acquired resistance to clinical cancer therapy: a twist in physiological signaling. Physiol Rev 2016;96:805-29.
29. Zhang Y, Zhang XO, Chen T et al. Circular intronic long noncoding RNAs. Mol Cell 2013;51:792-806.
30. Chen X, Chen RX, Wei WS et al. PRMT5 circular RNA promotes metastasis of urothelial carcinoma of the bladder through sponging miR-30c to induce epithelial–mesenchymal transition. Clin Cancer Res 2018;24:6319-30.
31. Ding Z, Guo L, Deng Z, Li P. Circ-PRMT5 enhances the proliferation, migration and glycolysis of hepatoma cells by targeting miR-188-5p/HK2 axis. Ann Hepatol 2020;19:269-79.
32. Du W, Li D, Guo X et al. Circ-PRMT5 promotes gastric cancer progression by sponging miR-145 and miR-1304 to upregulate MYC. Artif Cells Nanomed Biotechnol 2019;47:4120-30.
33. Zhang C, Zhang C, Lin J, Wang H. Circular RNA Hsa_Circ_0091579 serves as a diagnostic and prognostic marker for hepatocellular carcinoma. Cell Physiol Biochem 2018;51:290-300.
34. Yu C, Wang M, Li Z et al. MicroRNA-138-5p regulates pancreatic cancer cell growth through targeting FOXC1. Cell Oncol (Dordr) 2015;38:173-81.
35. Li J, Wang Q, Wen R et al. MiR-138 inhibits cell proliferation and reverses epithelial-mesenchymal transition in non-small cell lung cancer cells by targeting GIT 1 and SEMA 4C. J Cell Mol Med 2015;19:2793-805.
36. Gao Y, Fan X, Li W et al. miR-138-5p reverses gefitinib resistance in non-small cell lung cancer cells via negatively regulating G protein-coupled receptor 124. Biochem Biophys Res Commun 2014;446:179-86.
37. Jin Z, Guan L, Song Y, Xiang GM, Chen SX ,Gao B. MicroRNA-138 regulates chemoresistance in human non-small cell lung cancer via epithelial mesenchymal transition. Eur Rev Med Pharmacol Sci 2016;20:1080-6.
38. Felekkis K, Touvana E, Stefanou C, Deltas C. microRNAs: a newly described class of encoded molecules that play a role in health and disease. Hippokratia 2010;14:236.
39. Sur D, Coza O, Havasi A et al. Exosomal miRNAs in colorectal cancer: the carriers of useful news. J BUON 2020;25:23-34.
40. Lajos R, Braicu C, Jurj A et al. A miRNAs profile evolution of triple negative breast cancer cells in the presence of a possible adjuvant therapy and senescence inducer. J BUON 2018;23:692-705.
41. Liang S, He L, Zhao X et al. MicroRNA let-7f inhibits tumor invasion and metastasis by targeting MYH9 in human gastric cancer. PLoS One 2011;6:e18409.
42. Lin X, Yu G-F, Zuo S et al. Low MYH9 expression predicts a good prognosis for hepatocellular carcinoma. Int J Clin Exp Pathol 2018;11:2784-91.
43. Liu L, Yi J, Deng X et al. MYH9 overexpression correlates with clinicopathological parameters and poor prognosis of epithelial ovarian cancer. Oncol Lett 2019;18:1049-56.
44. Katono K, Sato Y, Jiang S-X et al. Prognostic significance of MYH9 expression in resected non-small cell lung cancer. PLoS One 2015;10:e0121460.